Final version published as: Grayli, S. V., Leach, G. W., Bahreyni, B. Sol-Gel Deposition and Characterization of 1 Vanadium Pentoxide Thin Films with High TCR. *Sensors and Actuators A: Physical* v. 279 (2018). 630-637. https://doi.org/10.1016/j.sna.2018.07.002

Sol-Gel Deposition and Characterization of Vanadium Pentoxide Thin Films with High TCR

Siamack V. Grayli[⊥], *Gary W. Leach*[╫], *and Behraad Bahreyni*[⊥]

[⊥]School of Mechatronic Systems Engineering, Simon Fraser University, Surrey, Canada

[╫]Department of Chemistry, Simon Fraser University, Burnaby, Canada

{svgrayli, gleach, bba19}@sfu.ca

Abstract

Vanadium pentoxide thin films have been deposited on quartz substrates via sol-gel synthesis and dip coating. The process was developed to establish a reliable and inexpensive method to produce thin films with a high temperature coefficient of resistance (TCR) for sensing applications. Sol-gel precursor concentration and post-deposition annealing conditions were varied to address their effects on film composition, morphology, structure, resistivity, and TCR response. The resulting thin films were structurally characterized by thin film profilometry, x-ray diffraction, scanning electron microscopy, and Raman spectroscopy. Resistivity and TCR measurements were carried out to determine their efficacy as sensor materials. Both low and high concentration alkoxide sol-gel precursors led to films of pure α-V_2O_5 composition but with characteristically different structural and electrical properties. Low concentration films showed a modest decrease in resistivity and TCR with increasing annealing temperature, consistent with the formation of increasing grain size and the coalescence of largely planar grains with common crystalline orientation. In contrast, films fabricated from higher alkoxide precursor

concentration are characterized by a higher density of grains with a larger dispersion in orientation and better-developed grain boundaries, leading to a general increase in resistivity and TCR with annealing temperature. The TCR of the films lied in the range of -3%°C^{-1} to -4%°C^{-1}, comparing favorably with films produced through conventional techniques such as DC magnetron sputtering, chemical vapor deposition, or pulsed laser deposition. Further, their TCR and resistivity characteristics can be controlled through sol-gel precursor concentration and post-deposition annealing temperature, indicating that sol-gel deposited vanadium pentoxide films are promising candidates for infrared sensor applications.

1 Introduction

Vanadium oxide has been the focus of widespread interest in industry and academia for its outstanding physical properties which include an insulator-to-metal phase transition [1], [2], reversible or irreversible crystalline lattice changes during thermal annealing [3]–[5], and a high temperature coefficient of resistance (TCR) [2], [6]. The high TCR of vanadium oxide has resulted in its use in room-temperature infrared sensing applications [7]–[10]. A broad review of the common deposition techniques distinguishes between traditional vacuum methods that require a cleanroom setup for accomplishing the task versus room temperature methods whereby the deposition occurs through chemical processes that are carried at the ambient temperature. Variations of physical deposition techniques such as reactive ion beam sputtering, RF sputtering and e-beam evaporation are some of the most commonly employed methods to deposit vanadium oxide thin films [11]–[14]. The majority of these techniques produce films with TCR values in the range of -2%°C^{-1} to -3%°C^{-1}. Recent works in the field such as [15], [16] have reported -3.5%°C^{-1} and -2.8%°C^{-1} TCR respectively. Amid the high uniformity of the deposited thin films, these methods bear high fabrication costs which are associated with cleanroom usage while offering limited increase in the TCR of the deposited thin films beyond the reported values. Concurrently, vacuum deposition methods cannot achieve stoichiometric compositions

of vanadium oxide layers due to the existence of multiple phases in the vanadium oxygen phase diagram, therefore crystalline systems resulting from vacuum deposition methods result in sub-stoichiometric vanadium-oxygen crystalline structures that may result in less stable materials [5], [17]. These techniques, also, yield little control over the oxidation state of the deposited films and often create mixed oxide phases which can undergo physical phase transitions as the device heats up when irradiated by incident IR radiation [18]–[20]. Physical phase transitions, aside from introducing mechanical stress in the thin film, affect the charge transport characteristics of the thin film vanadium oxide [5]. Other phenomena such as the insulator-to-metal transition in VO_2 can also introduce abrupt changes in the deposited materials electrical properties over a narrow temperature range which can be undesirable for sensing applications above room temperature [5].

Both recently and in the past, researchers have investigated room temperature deposition methods such as spray pyrolysis, spin coating, drop casting and dip coating [21]–[24]. Due to the nature of the deposition techniques, these methods use a precursor that is synthesized prior to the thin film deposition. The TCR values for as-deposited thin films this way are not comparable to those from the vacuum techniques hence high temperature annealing is needed to increase the TCR values of the deposited films. Some of the recent works in the field are reported by [25], [26] with TCR values of $-1.4\%°C^{-1}$ and $-2\%°C^{-1}$ for the as-deposited films. Annealing however increases the TCR values significantly. Of the two most studied cases, vanadium dioxide (VO_2) offers relatively higher TCR ($\sim -4\%°C^{-1}$) yet is less stable whereas vanadium pentoxide (V_2O_5) offers slightly lower TCR ($\sim -3.5\%°C^{-1}$) but is chemically stable [17], [25], [26]. Higher density of vanadium oxygen bonds in V_2O_5 results in broader IR absorption spectra hence make the material a more suitable choice for RT IR sensing applications [27]–[29]. It is therefore important to investigate methods to deposit vanadium pentoxide thin films with high purity that are not hampered by the mix oxide phase composition and Vanadium oxide has been the

focus of widespread interest in industry and academia for its outstanding physical properties which include an insulator-to-metal phase transition [1], [2], reversible or irreversible crystalline lattice changes during thermal annealing [3]–[5], and a high temperature coefficient of resistance (TCR) [2], [6]. The high TCR of vanadium oxide has resulted in its use in room-temperature infrared sensing applications [7]–[10]. A broad review of the common deposition techniques distinguishes between traditional vacuum methods that require a cleanroom setup for accomplishing the task versus room temperature methods whereby the deposition occurs through chemical processes that are carried at the ambient temperature. Variations of physical deposition techniques such as reactive ion beam sputtering, RF sputtering and e-beam evaporation are some of the most commonly employed methods to deposit vanadium oxide thin films [11]–[14]. The majority of these techniques produce films with TCR values in the range of $-2\%°C^{-1}$ to $-3\%°C^{-1}$. Recent works in the field such as [15], [16] have reported $-3.5\%°C^{-1}$ and $-2.8\%°C^{-1}$ TCR respectively. Amid the high uniformity of the deposited thin films, these methods bear high fabrication costs which are associated with cleanroom usage while offering limited increase in the TCR of the deposited thin films beyond the reported values. Concurrently, vacuum deposition methods cannot achieve stoichiometric compositions of vanadium oxide layers due to the existence of multiple phases in the vanadium oxygen phase diagram, therefore crystalline systems resulting from vacuum deposition methods result in sub-stoichiometric vanadium-oxygen crystalline structures that may result in less stable materials [5], [17]. These techniques, also, yield little control over the oxidation state of the deposited films and often create mixed oxide phases which can undergo physical phase transitions as the device heats up when irradiated by incident IR radiation [18]–[20]. Physical phase transitions, aside from introducing mechanical stress in the thin film, affect the charge transport characteristics of the thin film vanadium oxide [5]. Other phenomena such as the insulator-to-metal transition in VO_2 can also introduce abrupt changes in the deposited materials electrical properties over

a narrow temperature range which can be undesirable for sensing applications above room temperature [5].

Both recently and in the past, researchers have investigated room temperature deposition methods such as spray pyrolysis, spin coating, drop casting and dip coating [21]–[24]. Due to the nature of the deposition techniques, these methods use a precursor that is synthesized prior to the thin film deposition. The TCR values for as-deposited thin films this way are not comparable to those from the vacuum techniques hence high temperature annealing is needed to increase the TCR values of the deposited films. Some of the recent works in the field are reported by [25], [26] with TCR values of -1.4%°C^{-1} and -2%°C^{-1} for the as-deposited films. Annealing, however, can increase the TCR values significantly to about -4% [26]. Of the two most studied cases, vanadium dioxide (VO_2) offers relatively higher TCR (~ -4%°C^{-1}) yet is less stable whereas vanadium pentoxide (V_2O_5) offers slightly lower TCR (~ -3.5%°C^{-1}) but is chemically stable [17], [25], [26]. Higher density of vanadium oxygen bonds in V_2O_5 results in broader IR absorption spectra hence make the material a more suitable choice for RT IR sensing applications [27]–[29]. It is therefore important to investigate methods to deposit vanadium pentoxide thin films with high purity that are not hampered by the mix oxide phase composition and offer a broader IR absorption range for sensing applications [27], [28]. Previous research has demonstrated the possibility of solution phase chemistry, such as sol-gel processes, for the synthesis of vanadium oxide and deposition methods such as dip coating or spray coating of non-planar surfaces to improve process repeatability [30]–[32]. Our work provides a thorough investigation of the development of high purity phase crystalline vanadium pentoxide thin films as well as a full structural and electrical characterization of the deposited films as a function of precursor concentration and temperature. Table 1 offers a comparison between what presented here and the previous work in the field.offer a broader IR absorption range for sensing applications [27], [28]. Previous research has demonstrated the possibility

of solution phase chemistry, such as sol-gel processes, for the synthesis of vanadium oxide and deposition methods such as dip coating or spray coating of non-planar surfaces to improve process repeatability [30]–[32]. Our work provides a thorough investigation of the development of high purity phase crystalline vanadium pentoxide thin films as well as a full structural and electrical characterization of the deposited films as a function of precursor concentration and temperature. Table 1 offers a comparison between what presented here and the previous work in the field.

Table 1 Summary of the previous works in the field and its comparison with the current work

Reference	Material	Deposition Method	Deposition Temp [°C]	Reported TCR [%]	Resistivity [Ω-cm]	Annealing Conditions
Current Study	V_2O_5	Sol-Gel/Dip Coating	Room temp	-2.5 to -4.4	0.17 – 14	[300,400,500,650]°C for 6 ½ h
[21]	V_2O_5	Spray Pyrolysis	Room temp	Not-Reported	1.206	500 ° C for 1h
[22]	VO_2	Sputtering	Not-Reported	Not-Reported	358	400°C for 1h
[33]	V_2O_5	Atomic Layer Dep.	75 - 250	Not-Reported	Not-Reported	[250, 450, 700] ° C
[34]	V_2O_5 Gel	Inkjet Printing	Room temp	Not-Reported	Not-Reported	Not-Reported
[35]	VO_2 / V_3O_6 mix	Reactive Ion Beam	250 - 550	Not-Reported	0.5	Not-Reported
[15]	VO_2	e-beam Evaporation	26 - 300	-3.2	1.20	Not-Reported
[23]	V_2O_5	Spray Pyrolysis	Room temp	Not-Reported	500,000,000	Not Reported
[25]	VO_2/V_2O_5 Mix	Spray Pyrolysis	300 - 500	-4.6	0.2 – 2.8	500°C
[36]	VO_2	Sol-Gel/Dip Coat	Room temp	Not-Reported	2000	[110, 300, 500, 700] ° C for 1h
[26]	VO_2/V_2O_5 mix	Sol-Gel/Spin Coat	Room temp	-0.5	10,000	[530, 580] ° C for 2h
[37]	V_2O_5	Sol-Gel/Spin Coat	Room temp	-1.8 to -2.5	0.26 – 2.6	650 ° C for 6 ½ h

We previously reported typical TCR values of -2.0%°C^{-1} for thin samples of less than 200nm in thickness [37]. We also observed a thickness dependence of the TCR response as well as the resistivity of annealed samples to be generally larger than those not subject to annealing. However, our observations did not allow us to establish a well-defined link between sample thickness, TCR response, and film resistance. In this work, we present the use of sol-gel chemistry to synthesize pure phase vanadium pentoxide thin films. We have investigated the effects of alkoxide concentration in the pre-hydrolysis sol and film thickness as well as post-deposition film annealing on the formation of vanadium

oxide thin films. We also present measurements on the thermo-electrical response of the films, which exhibit high TCR values needed for RT IR detection.

2 Experimental

Thin films of vanadium oxide were deposited onto 0.5mm thick, 25mm×25mm square quartz slides. Prior to deposition, the slides were cleaned with powdered soap and coarse brushing, rinsed with deionized water, sonicated in acetone and isopropyl alcohol (IPA), each for 30 minutes. The substrates were placed in a 120ºC oven and dried over 24 hours prior to deposition to reduce uncontrolled hydrolytic condensation of the vanadium sol upon contact with the substrates.

The vanadium oxide thin films were deposited through controlled hydrolytic poly-condensation of vanadium tri-isopropoxide ($VO(OC_3H_7)_3$), purchased in liquid form from Sigma-Aldrich. The precursor was mixed with IPA to form the sol at room temperature. The prepared sol was then magnetically stirred for 30 minutes before dilution with an additional 10ml of IPA. The latter was added to ensure that poly-condensation would occur more homogeneously throughout the solution. The pH of the solution was measured three times during the following 120 minutes of stirring and ranged from 3.9 to 4.7. Thin film samples were prepared with two different alkoxide precursor concentrations. A low-concentration batch was carried out with an alkoxide concentration of 4.00v/v% whereas the high-concentration batch was carried out with a 25.33v/v%. The thin films deposited with the low-concentration and the high-concentration batches are referred to as low-concentration and high-concentration samples throughout the rest of the manuscript.

The poly-condensation of vanadium tri-isopropoxide occurs through a series of complex chain reactions that include the occurrence of both condensation and hydrolysis concurrently. The simplified reactions are given through [38–42]:

$$(C_3H_7O)_2OV(C_3H_7) + H_2O \rightarrow (OC_3H_7)_2OV(OH) + C_3H_7OH \quad (1)$$

$$(OC_3H_7)_2OV(OH) + (C_3H_7O)_2VO(OC_3H_7)_2 \rightarrow = (OV - O - VO) = +C_3H_7OH \quad (2)$$

The nature of these reactions and the condensation conditions as determined by the ratio of water to alkoxide present in the solution dictates the extent to which a long and condensed oxide network forms. This ratio can be utilized as a control measure over the density and complexity of the resulting oxide network. An automated dip coater was used to coat the substrates at the constant dip and withdrawal rates of 75mm/min. Films were deposited by immersing and withdrawing the substrates into the sol 7 times, with a 120 second wait time between each substrate dip, in order for the deposited layer to hydrolyze before subsequent immersion in the sol. In order to better understand the structural and conformational transitions of the vanadium oxide sol-gel films upon annealing, four samples from each concentration group were annealed at 4 different annealing temperatures (300°C, 400°C, 500°C, and 650°C) for 6½ hours in a high temperature furnace (Ney-Vulcan 3-550) while one sample from each group was kept "as-deposited" for reference.

2.1 STRUCTURAL CHARACTERIZATION

All samples underwent structural characterization to investigate the effects of various degrees of thermal annealing as well as the changes in the precursor alkoxide concentration on the microstructure of the deposited thin films. Sample surface roughness and film thickness parameters were measured using a Bruker Dektak XT profilometer. X-Ray diffraction studies were carried out using a Bruker D-8 Advance X-Ray diffractometer equipped with a Cu Kα source (λ=1.5406 Å) for 2θ angles between 10º and 90º at a scan rate of 0.02 °/s. Raman spectroscopy was carried out using a Renishaw Invia Raman spectrometer

and microscope. Surface morphology and grain structure of the deposited films were examined using an FEI-Nova NanoSEM scanning electron microscope at ×10k, ×30k and ×100k magnifications.

2.2 ELECTRICAL CHARACTERIZATION

Interdigitated comb electrodes (5 nm chromium + 150 nm gold) were deposited above the vanadium oxide films using a shadow mask and used for the electrical measurements. Each resistor had 14 fingers with 100μm width/gap connected alternatively to two contact pads. The electrical resistance of the samples was measured as a function temperature using a vacuum probe station with a heated chuck (Janis Research model RT-475K-4), a precise temperature controller (Scientific Instruments model 9700), and a source meter (Keithley model 2400) (see Figure 1). Sample electrical resistance measurements were carried out over the temperature range of 36°C to 72°C with a 0.5°C/min temperature ramp. We waited ~10 minutes after each temperature change for the sample to reach thermal equilibrium with the chuck.

FIGURE_01

3 Results and Discussion

Structural and electrical characterization of the resulting films provides a strong connection between vanadium oxide film quality and their resulting TCR and resistivity characteristics.

3.1 MORPHOLOGY AND STRUCTURE

Analysis of the average profile heights of the as-deposited and annealed films indicated a significant reduction in film thickness after the annealing step. The thickness of the as-deposited high-concentration

FIGURE_02

film is approximately twice the thickness of the as-deposited low-concentration film and both groups display a significant decrease in film thickness upon annealing, suggesting that the as-deposited films are relatively porous and undergo significant densification when annealed (Figure 2).

This difference in thickness can be associated with the difference in the precursor alkoxide concentration, as predicted by (1) and (2), since increasing the alkoxide concentration leads to a higher density of the hydrolyzed oxide network. Profilometry reveals that the average film thickness of the high and low-concentration films are approximately 400nm and 50nm after annealing, respectively.

Figure 3 shows scanning electron micrographs of the low and high-concentration films with the different annealing conditions. The as-deposited morphologies in both groups are characterized by continuous films with an amorphous structure, whereas both groups show a similar progression from smooth connective surface from as-deposited films to densely connected crystallites in the annealed ones. At temperatures 400°C and higher, the grain structures become prominent.

FIGURE_03

Despite the similarities in structure growth between the two groups, the 650°C annealed samples from the high-concentration group, show development of larger and more well-defined crystallites with well-developed grain boundaries. Additionally, there is an apparently larger number of crystallites and orientations in films from the high-concentration group than the low-concentration counterparts. Comparable in size and shape, the low-concentration group's 650°C annealed samples contain less densely packed crystallites which have coalesced to form preferentially grown connected networks in the (001) direction parallel to the substrate. These observations are in corroboration with the emergence of additional less intense peaks in the XRD patterns of the 650°C annealed samples from the high-concentration group. The XRD patterns for both the high and low-concentration 650°C annealed films

are shown in Figure 4. Also shown is a reference powder X-ray diffraction pattern of vanadium pentoxide (α-V_2O_5). The diffraction patterns of both the high and low-concentration samples are dominated by a single (001) diffraction peak at ~20.4º in 2θ, indicating that the sol-gel deposition and annealing protocol leads to the deposition of single phase α-V_2O_5 material that is highly oriented. Our data for films annealed at other temperatures reveal that the as-deposited films are nominally X-ray amorphous and increase their degree of crystallinity with annealing temperature, as indicated by an increasing (001) diffraction intensity in the XRD traces.

FIGURE_04

No indication of the formation of other structural forms or oxidation states of vanadium oxide is evident from the XRD data. The strong intensity in the (001) diffraction peak is an indicator of (ab) plane growth parallel to the substrate (Figure 4-right).

Notably, there are additional low-intensity diffraction peaks in the XRD pattern of the high-concentration samples which are not evident in the low-concentration group. These peaks are more prominent in samples that were annealed at 650°C than those annealed at lower temperatures but are nevertheless present in all high-concentration samples. The presence of a dominant (001) diffraction peak and, albeit weak, α-V_2O_5 diffraction peaks in the high-concentration samples indicates that the resulting high-concentration films, while highly oriented, are not quite as well oriented as the low-concentration films. This reaffirms that the high-concentration samples possess a larger range of crystallite orientations than do the low-concentration samples which are otherwise similar in crystallite composition.

FIGURE_05

FIGURE_06

Raman spectroscopy was employed to help identify the phase purity and degree of crystallinity of the deposited films and to investigate any effects as the result of the change in concentration of the alkoxide in the precursor sol. Well-defined Raman vibrational features begin to appear and grow in intensity for films annealed at higher temperatures which is an indicator of formation of larger and denser crystalline grain boundaries (see Figure 5). Consistent with the XRD observations, the high-concentration sample group shows stronger Raman signals than the corresponding low-concentration films but do not differ in other respects, indicating that the alkoxide precursor concentration has no effect on the resulting sol-gel chemistry or bonding structure in the final vanadium oxide films, but only results in an effective thickness or concentration effect on the final annealed films. The Raman modes appearing at 144, 196, (283, 303), 404, (480, 525), 699, and 993 wavenumbers, are consistent with previous observations of the lattice phonon mode structure of α-V_2O_5 [44]–[46] which contrasts the results reported for other fabrication methods such as physical vapor deposition (PVD) or pulsed laser deposition where other stable oxides of vanadium such as VO_2 and V_2O_3 form upon annealing.

3.2 ELECTRICAL PROPERTIES

Figure 6 summarizes the measured resistivity of the deposited thin films versus annealing conditions. The measurements were carried out at 46 ºC as described in order to allow the samples to reach thermal equilibrium with the heating chuck hence minimize the readout resistance fluctuations, and are plotted versus the sample annealing temperature. Similar plot for the room temperature resistances is added for comparison's sake. The as-deposited low and high-concentration samples display resistivity values of 5.6 Ω-cm and 8.7 Ω-cm, respectively. Annealing the films led to an increase in resistivity except for the low-concentration 650 ºC-annealed sample which exhibited a significant drop to a resistivity of 0.17 Ω-cm.

The resistivity of semiconducting transition metal oxides obeys a thermally activated hopping mechanism characterized by the following relationship [47], [48]:

$$\rho(T) = \rho_o e^{\left(\frac{E_a}{k_B T}\right)} \tag{3}$$

where ρ is the temperature dependent resistivity, ρ_o is the resistivity at infinite temperature, E_a is the charge carrier's activation energy, k_B is Boltzmann constant, and T is the temperature. Consequently, the temperature coefficient of resistance (TCR) of a resistor made from such a material, α, is calculated from [47], [48] :

$$\alpha = \frac{1}{R_0}\frac{\partial}{\partial T} R(T) = -\frac{E_a}{k_B} \cdot \frac{1}{T^2} \tag{4}$$

FIGURE_07

where R_0 is the resistance at infinite temperature. The TCR values for all the samples (annealed and as-deposited) in both low-concentration and high-concentration groups were calculated via fitting an exponential curve to the resistance measurements across a temperature range of 46–70°C with R^2 values of better than 0.99 for all fitted curves (see Figure 7). The results consistently demonstrated TCR values between -3% °C^{-1} and -4% °C^{-1} for different samples, compared to typical value of ~-2.5% °C^{-1} for films deposited through DC magnetron sputtering or pulsed laser deposition [6], [15], [49].

Evident from the measured electrical resistances (Figure 6) and the calculated TCR values (Figure 7), the low and high-concentration samples follow different trends in value as the annealing temperature of the samples increases from 300°C to 650°C. With an annealing temperature of 300°C, low-concentration samples exhibited higher electrical resistance than the high-concentration ones and their electrical resistance dropped significantly as the annealing temperature was increased to 650°C. For high-

concentration samples, however, the electrical resistance was lower for the samples annealed at 300°C against those annealed at 650°C. A similar trend is observed for the TCR values of the films. These trends can be explained by considering the structural differences between the two batches in the development of finer and more pronounced grain boundaries in the high-concentration samples as opposed to less densely packed and more coalesced crystallites with less well-defined grain boundaries in the low-concentration group (see Figure 3). Since V_2O_5 samples were developed in ambient conditions, they are sub-stoichiometric which indicates they contain oxygen vacancies that can serve as defect states for the proposed thermally activated hopping conduction within a given crystalline domain [5], [50]–[53]. In the absence of other barriers to charge migration, the formation of larger crystalline domains should favor increased conductivity and lower resistivity. However, the formation of grain boundaries and an associated inter-grain activation energy that is larger than the electron hopping barrier within single grains can impair charge carrier conduction across the sample and between grain boundaries as the samples from both groups become more poly-crystallized as a result of annealing. Therefore, we can attribute the resistivity in samples from both groups by the competing effects of grain size and grain boundary development with annealing. For transition metals, the material's TCR is reciprocally related to the electrical conductance and has a direct relationship with the charge carriers' activation energy through equation (4). In the case of the polycrystalline materials such as the one discussed by this work, the prevalent energy barrier to the charge carrier migration, are the crystalline grain boundaries that separate each crystalline domain from the other [54], [55].

Although annealing results in an increase in the density and the volume fraction of the crystallites in both sample groups, in low concentration samples, the annealing process causes the coalescence of the crystalline domains and lowers the density of well-defined grain boundaries, which in turns lowers the activation energy that is required for the electrons to overcome the energy barrier. This process results in

lowering of the TCR values as a function of annealing temperature. In the case of the high concentration samples, the grain boundaries are much more well-defined and spread abundantly across the thin film's surface. As a result, annealing in those samples results in an increase in the thin film's TCR through increasing the activation energy required for conductance [56]–[58].

The trends observed can attest that the opposing mechanisms at work can yield an optimum ground for a choice between the material concentration translated into thickness and the annealing temperature. For sensor applications that require CMOS compatibility hence low processing temperatures, low material concentration specimens can be used that yield very high TCR in as-deposited form.

Conclusions

We have demonstrated that vanadium pentoxide thin films synthesized via the sol-gel method and deposited through dip coating exhibit high TCR values, making them suitable for infrared sensing applications. We have investigated the effects of the concentration of the alkoxide precursor and post-deposition annealing temperature on morphology and electrical response of the devices. It was observed that the alkoxide concentration during the sol synthesis significantly affected the geometrical and crystalline structure of the grown films. In both groups, the crystallites demonstrated a preferential layered growth with the crystalline basal layer parallel to the substrate. However, crystallites formed in the low concentration films were more oriented than those in the higher concentration films leading to the formation of connected crystallites with larger grains for low alkoxide concentration against more densely packed crystallites with well-defined facets and grain boundaries for the higher alkoxide concentration. Accordingly, the resistivity and TCR properties of the samples prepared with different alkoxide concentration displayed opposite trends with annealing temperature, indicating that their electrical properties could be tuned by appropriate selection of sol precursor concentration and post-

deposition annealing conditions. The use of sol-gel deposited V_2O_5 is a promising approach to the development of low-cost IR sensors.

Acknowledgments

This project was supported by the Natural Sciences and Engineering Research Council of Canada (NSERC) through Automotive Partnership Canada projects. Access to engineering software was provided through CMC Microsystems. This work made use of 4D LABS shared facilities supported by the Canada Foundation for Innovation (CFI), British Columbia Knowledge Development Fund (BCKDF) and Simon Fraser University. The authors would like to acknowledge Dr. Xin Zhang for assistance in acquiring the scanning electron micrographs for the purpose of this study.

REFERENCES

[1] V. R. Morrison *et al.*, "A photoinduced metal-like phase of monoclinic VO2 revealed by ultrafast electron diffraction," *Science*, vol. 346, no. 6208, pp. 445–448, 2014.
[2] C. Venkatasubramanian, O. M. Cabarcos, D. L. Allara, M. W. Horn, and S. Ashok, "Correlation of temperature response and structure of annealed VO x thin films for IR detector applications," *J. Vac. Sci. Technol. Vac. Surf. Films*, vol. 27, no. 4, pp. 956–961, 2009.
[3] Z. . El Mandouh and M. . Selim, "Physical properties of vanadium pentoxide sol gel films," *Thin Solid Films*, vol. 371, no. 1–2, pp. 259–263, Aug. 2000.
[4] J. Livage, "Optical and electrical properties of vanadium oxides synthesized from alkoxides," *Coord. Chem. Rev.*, vol. 190–192, pp. 391–403, Sep. 1999.
[5] B. D. Gauntt, E. C. Dickey, and M. W. Horn, "Stoichiometry and microstructural effects on electrical conduction in pulsed dc sputtered vanadium oxide thin films," *J. Mater. Res.*, vol. 24, no. 04, pp. 1590–1599, 2009.
[6] N. Fieldhouse, S. M. Pursel, M. W. Horn, and S. S. N. Bharadwaja, "Electrical properties of vanadium oxide thin films for bolometer applications: processed by pulse dc sputtering," *J. Phys. Appl. Phys.*, vol. 42, no. 5, p. 055408, Mar. 2009.
[7] F. Niklaus, C. Vieider, and H. Jakobsen, "MEMS-based uncooled infrared bolometer arrays: a review," in *MEMS/MOEMS technologies and applications III*, 2008, vol. 6836, p. 68360D.
[8] M. S. de Castro, C. L. Ferreira, and R. R. de Avillez, "Vanadium oxide thin films produced by magnetron sputtering from a V2O5 target at room temperature," *Infrared Phys. Technol.*, vol. 60, pp. 103–107, 2013.
[9] A. Rogalski, *Infrared Detectors, Second Edition*. CRC Press, 2010.
[10] H. Budzier and G. Gerlach, *Thermal Infrared Sensors: Theory, Optimisation and Practice*. John Wiley & Sons, 2011.

[11] H. A. Basantani *et al.*, “Enhanced electrical and noise properties of nanocomposite vanadium oxide thin films by reactive pulsed-dc magnetron sputtering,” *Appl. Phys. Lett.*, vol. 100, no. 26, p. 262108, 2012.
[12] P. Wang *et al.*, “High Sensitivity $17 \mu \textm$ Pixel Pitch 640×512 Uncooled Infrared Focal Plane Arrays Based on Amorphous Vanadium Oxide Thin Films,” *IEEE Electron Device Lett.*, vol. 36, no. 9, pp. 923–925, Sep. 2015.
[13] S. S. N. Bharadwaja *et al.*, “Processing issues in pulse DC sputtering of vanadium oxide thin films for uncooled infrared detectors,” *Adv. Electroceramic Mater. II Vol. 221*, pp. 177–185, 2010.
[14] M. S. de Castro, C. L. Ferreira, and R. R. de Avillez, “Vanadium oxide thin films produced by magnetron sputtering from a V 2 O 5 target at room temperature,” *Infrared Phys. Technol.*, vol. 60, pp. 103–107, 2013.
[15] A. Subrahmanyam, Y. Bharat Kumar Redd, and C. L. Nagendra, “Nano-vanadium oxide thin films in mixed phase for microbolometer applications,” *J. Phys. Appl. Phys.*, vol. 41, no. 19, p. 195108, Oct. 2008.
[16] G. M. Gouda and C. L. Nagendra, “Preparation and characterization of thin film thermistors of metal oxides of manganese and vanadium (Mn-VO),” *Sens. Actuators Phys.*, vol. 190, pp. 181–190, 2013.
[17] Q. Su, W. Lan, Y. Y. Wang, and X. Q. Liu, “Structural characterization of β-V 2 O 5 films prepared by DC reactive magnetron sputtering,” *Appl. Surf. Sci.*, vol. 255, no. 7, pp. 4177–4179, 2009.
[18] P. Guggilla, A. K. Batra, J. R. Currie, M. D. Aggarwal, M. A. Alim, and R. B. Lal, “Pyroelectric ceramics for infrared detection applications,” *Mater. Lett.*, vol. 60, no. 16, pp. 1937–1942, 2006.
[19] L. Becker, “Influence of IR sensor technology on the military and civil defense,” in *Integrated Optoelectronic Devices 2006*, 2006, pp. 61270S–61270S.
[20] J. Narayan and V. M. Bhosle, “Phase transition and critical issues in structure-property correlations of vanadium oxide,” *J. Appl. Phys.*, vol. 100, no. 10, p. 103524, 2006.
[21] N. M. Abd-Alghafour, N. M. Ahmed, and Z. Hassan, “Fabrication and characterization of V2O5 nanorods based metal–semiconductor–metal photodetector,” *Sens. Actuators Phys.*, vol. 250, pp. 250–257, 2016.
[22] G. M. Gouda and C. L. Nagendra, “Structural and electrical properties of mixed oxides of manganese and vanadium: a new semiconductor oxide thermistor material,” *Sens. Actuators Phys.*, vol. 155, no. 2, pp. 263–271, 2009.
[23] Y. Vijayakumar *et al.*, “V2O5 nanofibers: Potential contestant for high performance xylene sensor,” *J. Alloys Compd.*, vol. 731, pp. 805–812, 2018.
[24] I. G. Madida *et al.*, “Submicronic VO2–PVP composites coatings for smart windows applications and solar heat management,” *Sol. Energy*, vol. 107, pp. 758–769, 2014.
[25] M. Benkahoul, M. K. Zayed, A. Solieman, and S. N. Alamri, “Spray deposition of V4O9 and V2O5 thin films and post-annealing formation of thermochromic VO2,” *J. Alloys Compd.*, vol. 704, pp. 760–768, 2017.
[26] L. N. Son, T. Tachiki, and T. Uchida, “Characteristics of vanadium oxide thin films prepared by metal–organic decomposition for bolometer detectors,” *Jpn. J. Appl. Phys.*, vol. 50, no. 2R, p. 025803, 2011.
[27] Y. J. Park, K. S. Ryu, N.-G. Park, Y.-S. Hong, and S. H. Chang, “RF-Sputtered Vanadium Oxide Films Effect of Film Thickness on Structural and Electrochemical Properties,” *J. Electrochem. Soc.*, vol. 149, no. 5, pp. A597–A602, 2002.

[28] S. Guimond *et al.*, "Well-ordered V2O5 (001) thin films on Au (111): growth and thermal stability," *J. Phys. Chem. C*, vol. 112, no. 31, pp. 11835–11846, 2008.
[29] K. R. Asmis and J. Sauer, "Mass-selective vibrational spectroscopy of vanadium oxide cluster ions," *Mass Spectrom. Rev.*, vol. 26, no. 4, pp. 542–562, 2007.
[30] C. Q. Feng, S. Y. Wang, R. Zeng, Z. P. Guo, K. Konstantinov, and H. K. Liu, "Synthesis of spherical porous vanadium pentoxide and its electrochemical properties," *J. Power Sources*, vol. 184, no. 2, pp. 485–488, Oct. 2008.
[31] C. Julien, J. P. Guesdon, A. Gorenstein, A. Khelfa, and I. Ivanov, "The influence of the substrate material on the growth of V2O5 flash-evaporated films," *Appl. Surf. Sci.*, vol. 90, no. 3, pp. 389–391, Nov. 1995.
[32] R. S. Ingole and B. J. Lokhande, "Nanoporous vanadium oxide network prepared by spray pyrolysis," *Mater. Lett.*, vol. 168, pp. 95–98, 2016.
[33] T. Blanquart *et al.*, "Atomic layer deposition and characterization of vanadium oxide thin films," *RSC Adv.*, vol. 3, no. 4, pp. 1179–1185, 2013.
[34] C. Costa, C. Pinheiro, I. Henriques, and C. A. Laia, "Electrochromic properties of inkjet printed vanadium oxide gel on flexible polyethylene terephthalate/indium tin oxide electrodes," *ACS Appl. Mater. Interfaces*, vol. 4, no. 10, pp. 5266–5275, 2012.
[35] K. G. West *et al.*, "Growth and characterization of vanadium dioxide thin films prepared by reactive-biased target ion beam deposition," *J. Vac. Sci. Technol. Vac. Surf. Films*, vol. 26, no. 1, pp. 133–139, 2008.
[36] Q. Shi *et al.*, "Preparation and phase transition characterization of VO2 thin film on single crystal Si (100) substrate by sol–gel process," *J. Sol-Gel Sci. Technol.*, vol. 59, no. 3, p. 591, 2011.
[37] S. V. Grayli, I. El-Chami, B. Bahreyni, and G. Leach, "Room temperature deposition of highly sensitive vanadium oxide films for infrared light sensing applications," in *SENSORS, 2015 IEEE*, Busan, South Korea, 2015, pp. 1–4.
[38] J. Livage, "Sol-gel chemistry and electrochemical properties of vanadium oxide gels," *Solid State Ion.*, vol. 86, pp. 935–942, 1996.
[39] J. Livage, "Vanadium pentoxide gels," *Chem Mater*, vol. 3, no. 4, pp. 578–593, 1991.
[40] J. Livage, "Optical and electrical properties of vanadium oxides synthesized from alkoxides," *Coord. Chem. Rev.*, vol. 190, pp. 391–403, 1999.
[41] F. P. Gökdemir, O. Özdemir, and K. Kutlu, "Comparison of Structural and Electrochemical Properties of V 2 O 5 Thin Films Prepared by Organic/Inorganic Precursors," *Electrochimica Acta*, vol. 121, pp. 240–244, 2014.
[42] N. Özer, "Electrochemical properties of sol-gel deposited vanadium pentoxide films," *Thin Solid Films*, vol. 305, no. 1–2, pp. 80–87, 1997.
[43] N. Das, H. Eckert, H. Hu, I. E. Wachs, J. F. Walzer, and F. J. Feher, "Bonding States of Surface Vanadium (V) Oxide Phases on Silica: Structural Characterization by^ 5^ 1V NMR and Raman Spectroscopy," *J. Phys. Chem.*, vol. 97, pp. 8240–8240, 1993.
[44] W. Avansi, L. J. Q. Maia, C. Ribeiro, E. R. Leite, and V. R. Mastelaro, "Local structure study of vanadium pentoxide 1D-nanostructures," *J. Nanoparticle Res.*, vol. 13, no. 10, p. 4937, 2011.
[45] P. Vilanova-Martínez, J. Hernández-Velasco, A. R. Landa-Cánovas, and F. Agulló-Rueda, "Laser heating induced phase changes of VO 2 crystals in air monitored by Raman spectroscopy," *J. Alloys Compd.*, vol. 661, pp. 122–125, 2016.
[46] S. Jagtap, S. Rane, U. Mulik, and D. Amalnerkar, "Thick film NTC thermistor for wide range of temperature sensing," *Microelectron. Int.*, vol. 24, no. 2, pp. 7–13, 2007.

[47] A. Feteira, “Negative temperature coefficient resistance (NTCR) ceramic thermistors: an industrial perspective,” *J. Am. Ceram. Soc.*, vol. 92, no. 5, pp. 967–983, 2009.
[48] F. Niklaus, C. Vieider, and H. Jakobsen, “MEMS-based uncooled infrared bolometer arrays: a review,” in *SPIE 6836, MEMS/MOEMS Technologies and Applications III, 68360D*, Beijing, China, 2007, p. 68360D.
[49] S. Somiya, *Handbook of advanced ceramics: materials, applications, processing, and properties*. Academic Press, 2013.
[50] L. Murawski, R. J. Barczynski, and A. Rybicka, “V2O5-P5O5 glass and its polaron transport properties derived from molecular dynamic simulations of structure,” in *dielectric and related phenomena: materials physico-chemistry, spectrometric investigations, and applications*, 1997, pp. 136–141.
[51] R. R. Heikes and W. D. Johnston, “Mechanism of Conduction in Li-Substituted Transition Metal Oxides,” *J. Chem. Phys.*, vol. 26, no. 3, pp. 582–587, 1957.
[52] J. B. Goodenough, “Narrow-band electrons in transition-metal oxides,” *Czechoslov. J. Phys. B*, vol. 17, no. 4, pp. 304–336, 1967.
[53] H. J. Avila-Paredes and S. Kim, “The effect of segregated transition metal ions on the grain boundary resistivity of gadolinium doped ceria: Alteration of the space charge potential,” *Solid State Ion.*, vol. 177, no. 35–36, pp. 3075–3080, 2006.
[54] X. Guo, W. Sigle, J. Fleig, and J. Maier, “Role of space charge in the grain boundary blocking effect in doped zirconia,” *Solid State Ion.*, vol. 154, pp. 555–561, 2002.
[55] K. Ellmer and R. Mientus, “Carrier transport in polycrystalline transparent conductive oxides: A comparative study of zinc oxide and indium oxide,” *Thin Solid Films*, vol. 516, no. 14, pp. 4620–4627, 2008.
[56] P. Lunkenheimer, S. Krohns, S. Riegg, S. G. Ebbinghaus, A. Reller, and A. Loidl, “Colossal dielectric constants in transition-metal oxides,” *Eur. Phys. J. Spec. Top.*, vol. 180, no. 1, pp. 61–89, 2009.
[57] T. W. Kelley and C. D. Frisbie, “Gate voltage dependent resistance of a single organic semiconductor grain boundary,” *J. Phys. Chem. B*, vol. 105, no. 20, pp. 4538–4540, 2001.

Figures

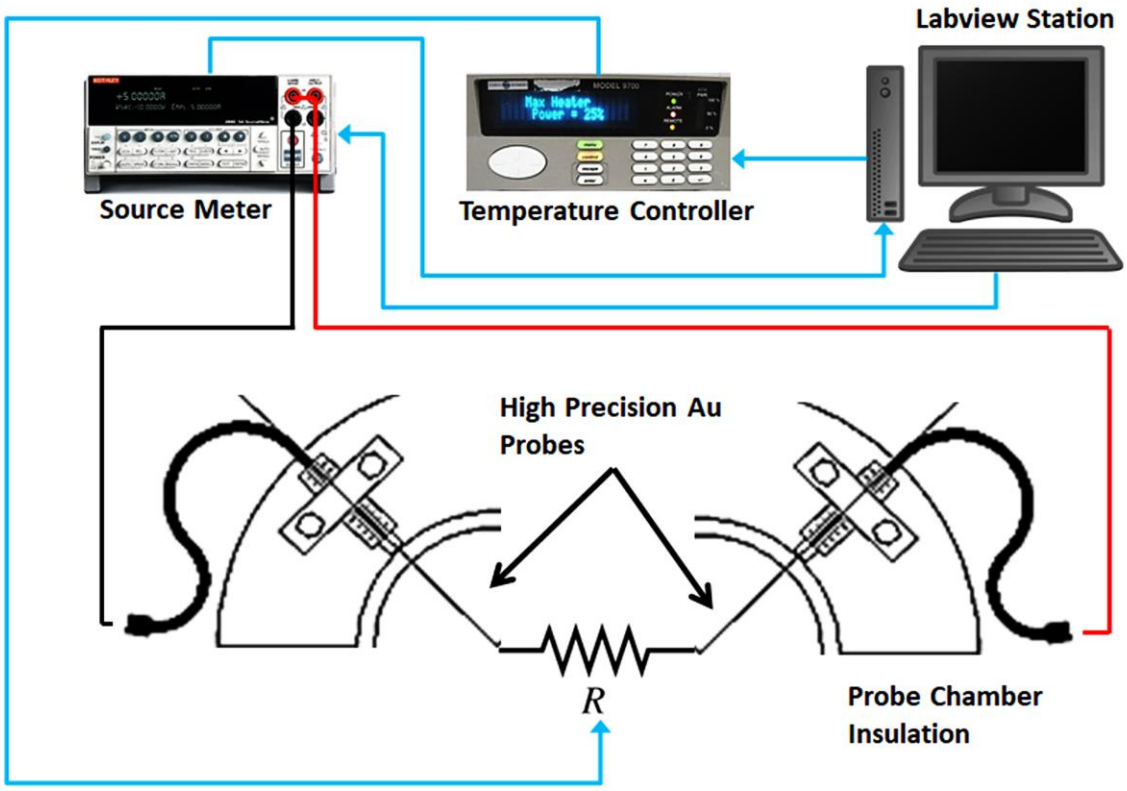

Figure 1 The schematic of the measurement setup that was used to characterize the electrical resistance of the samples as a function of temperature

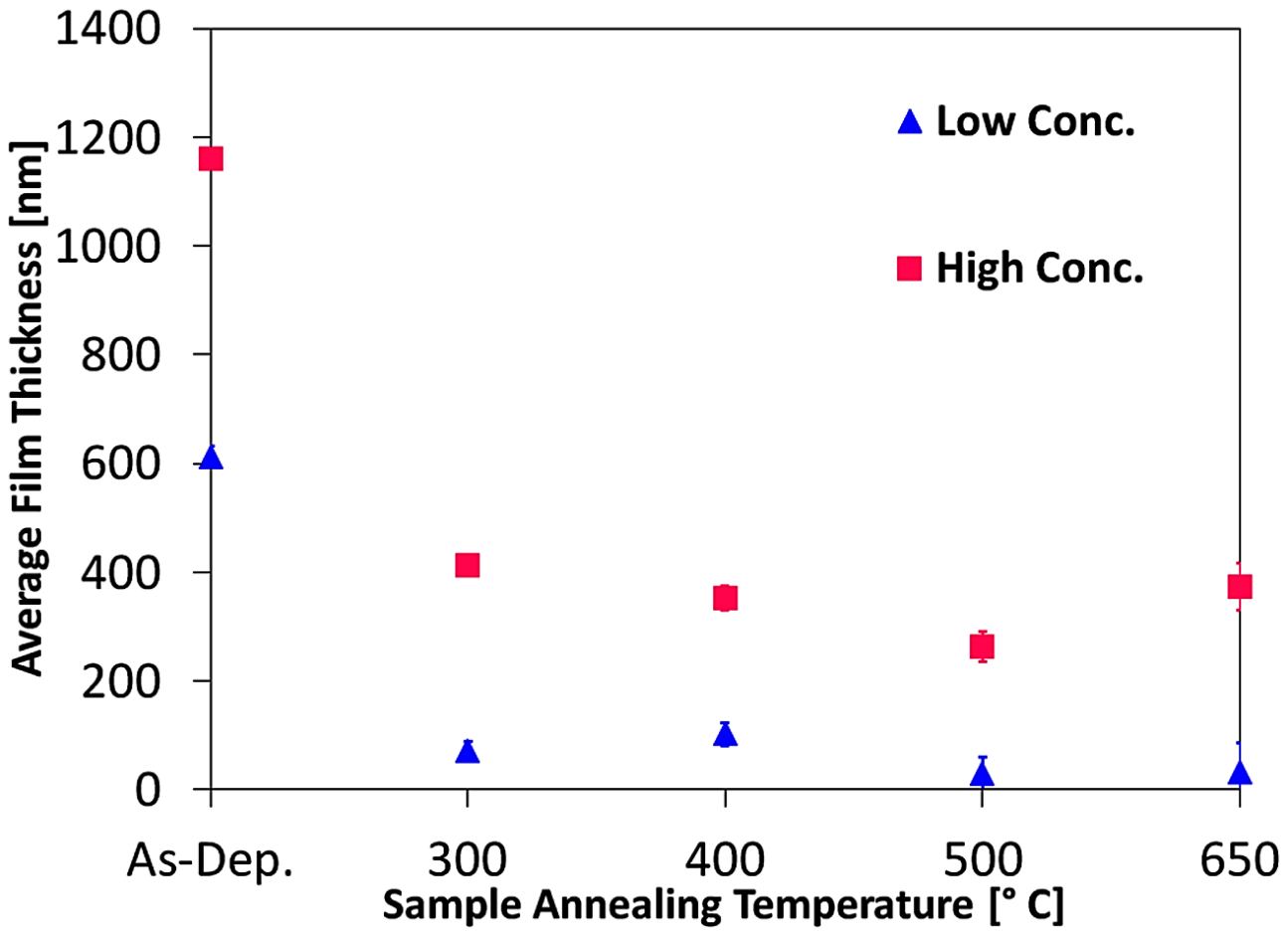

Figure 2 Film thickness (derived from the average profile height in profilometry data) versus the annealing temperature of the samples

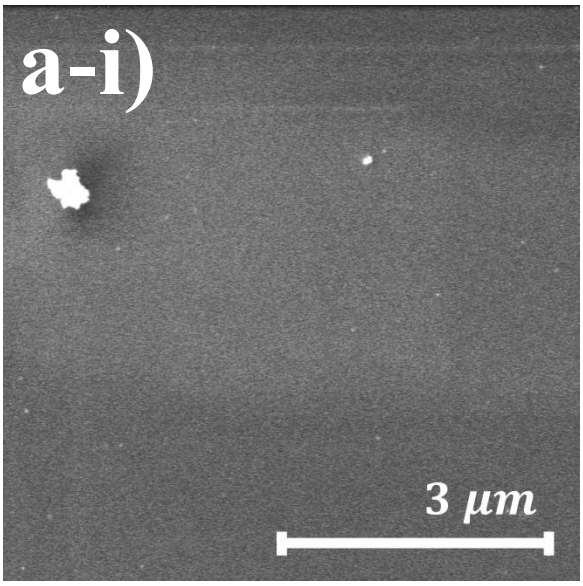
a-i)
3 μm

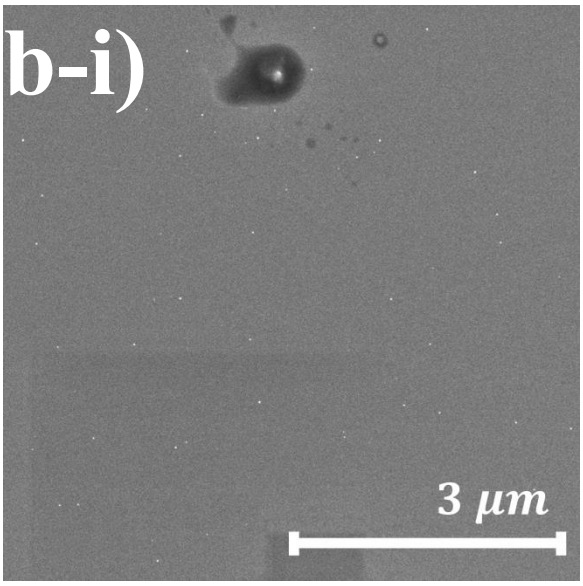
b-i)
3 μm

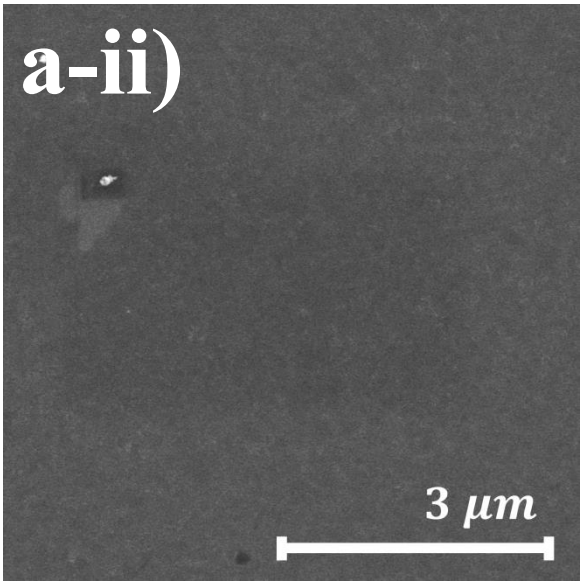
a-ii)
3 μm

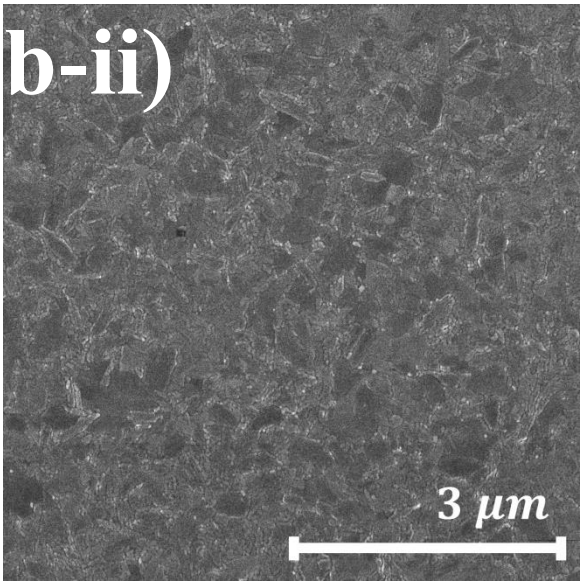
b-ii)
3 μm

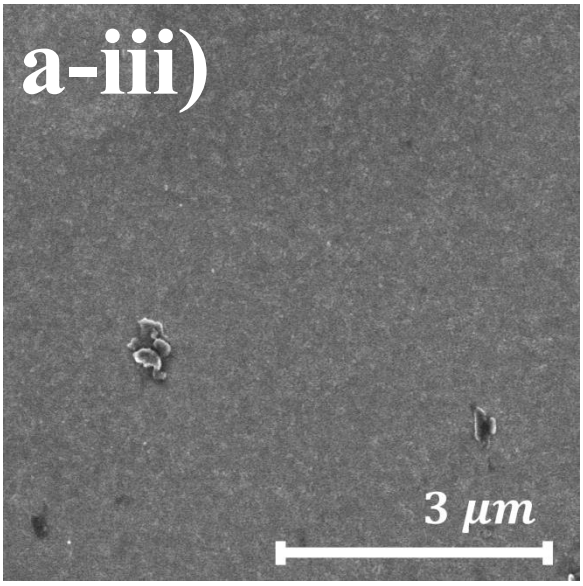
a-iii)
3 μm

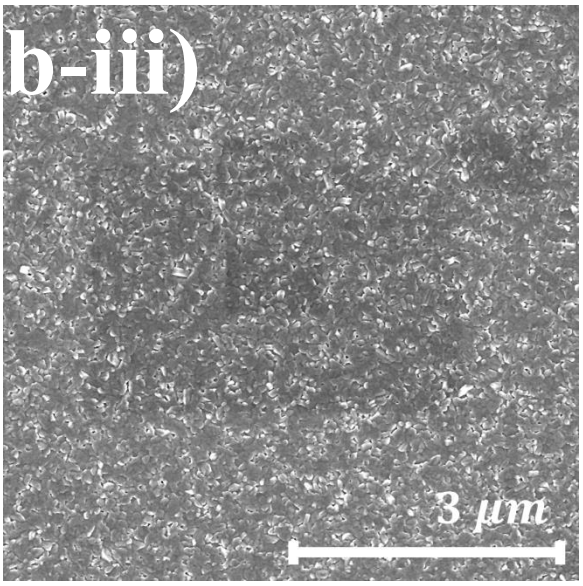
b-iii)
3 μm

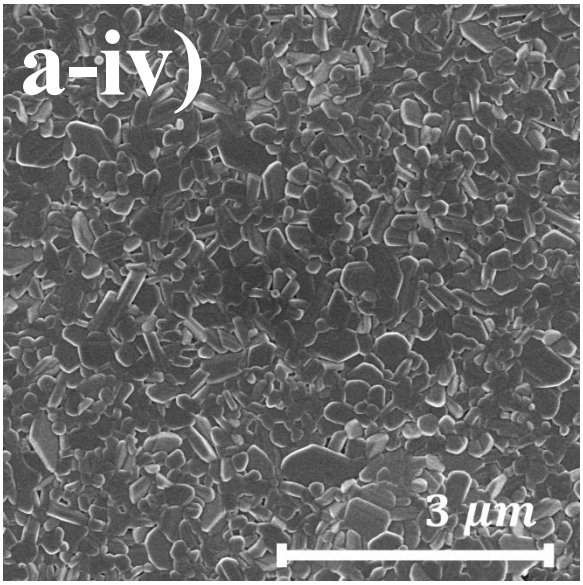
a-iv)
3 μm

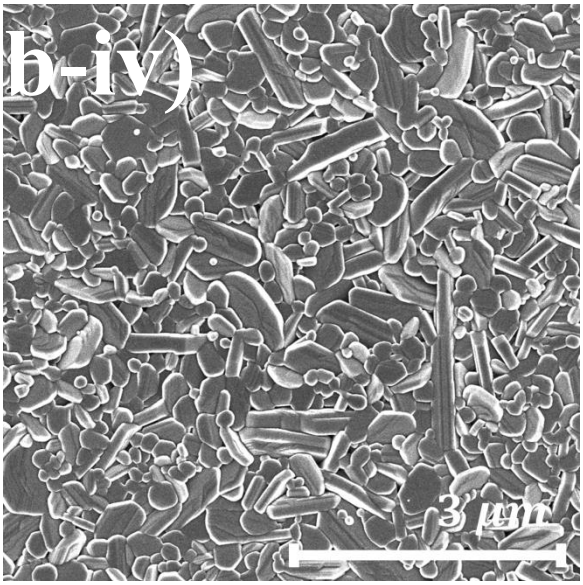
b-iv)
3 μm

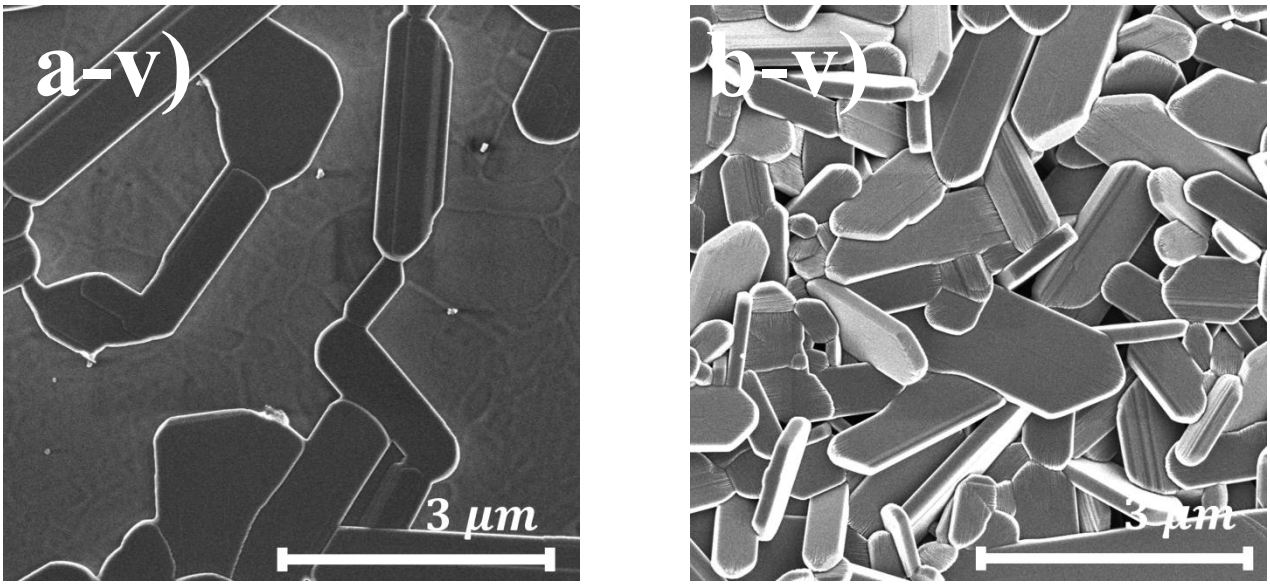

Figure 3 The SEM images of a-(i-v) Low concentration samples and b-(i-v) High concentration samples, annealed at 300°C, 400°C, 500°C and 650°C, respectively The highest resolution in either group (a-v and b-v) depict the sheet structural differences between the low and high concentration groups annealed at 650°C.

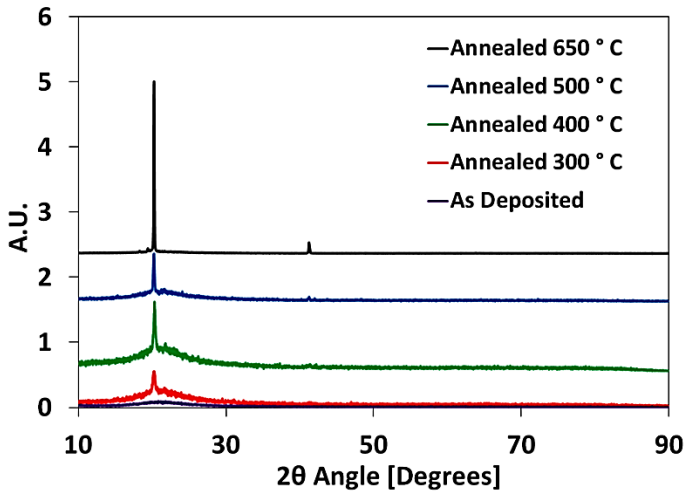

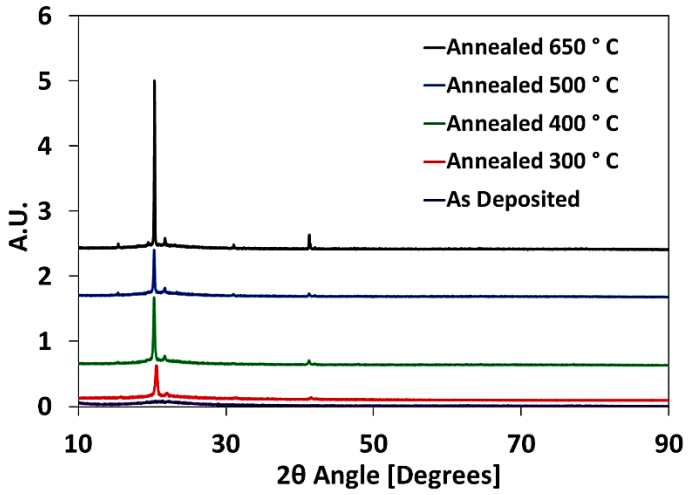

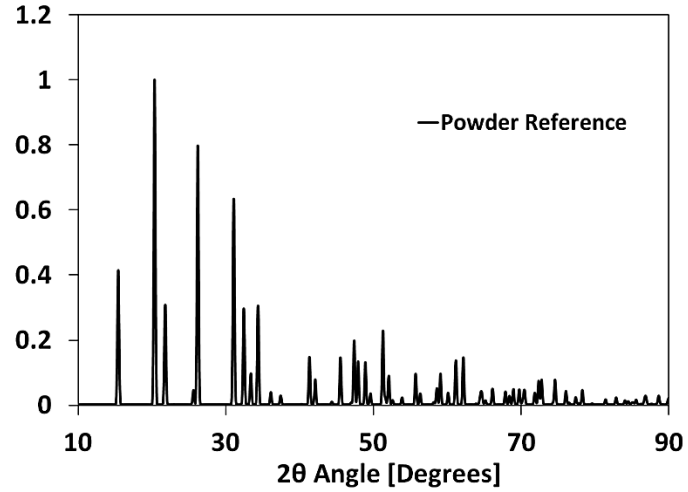

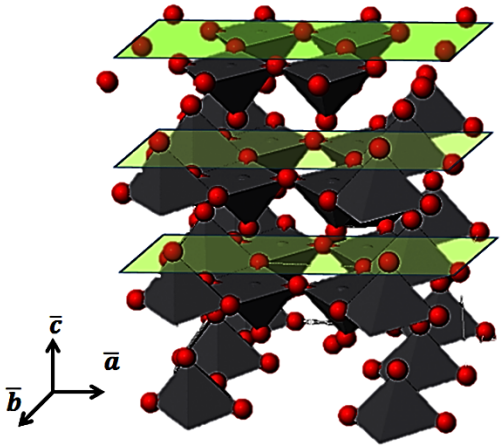

Figure 4 Left) The comparison between the XRD traces of low and high concentration samples (top and middle, respectively) annealed at different temperatures against powder reference of α-V_2O_5 (bottom).; Right) the layered structure of α-V_2O_5

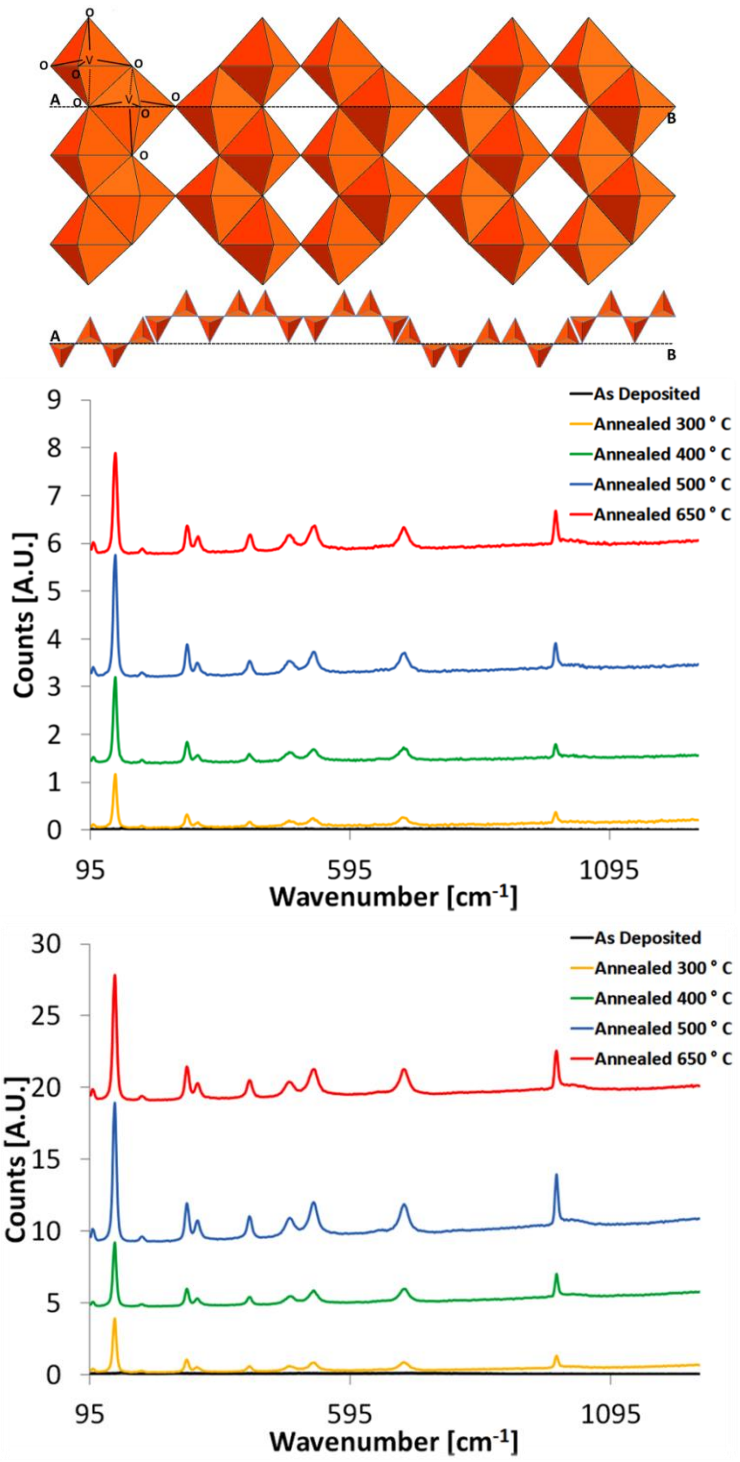

Figure 5Top) 2D view of the orthorhombic $\alpha - V_2O_5$ crystal lattice along the (001) direction where line AB depicts the crystal packing in the (010) direction. Raman spectra of low-concentration and high-concentration samples (middle and bottom, respectively) show identical characteristics with a nearly three-fold increase in the peak amplitudes associated with $\alpha - V_2O_5$ of the high-concentration group compared to the low-concentration ones

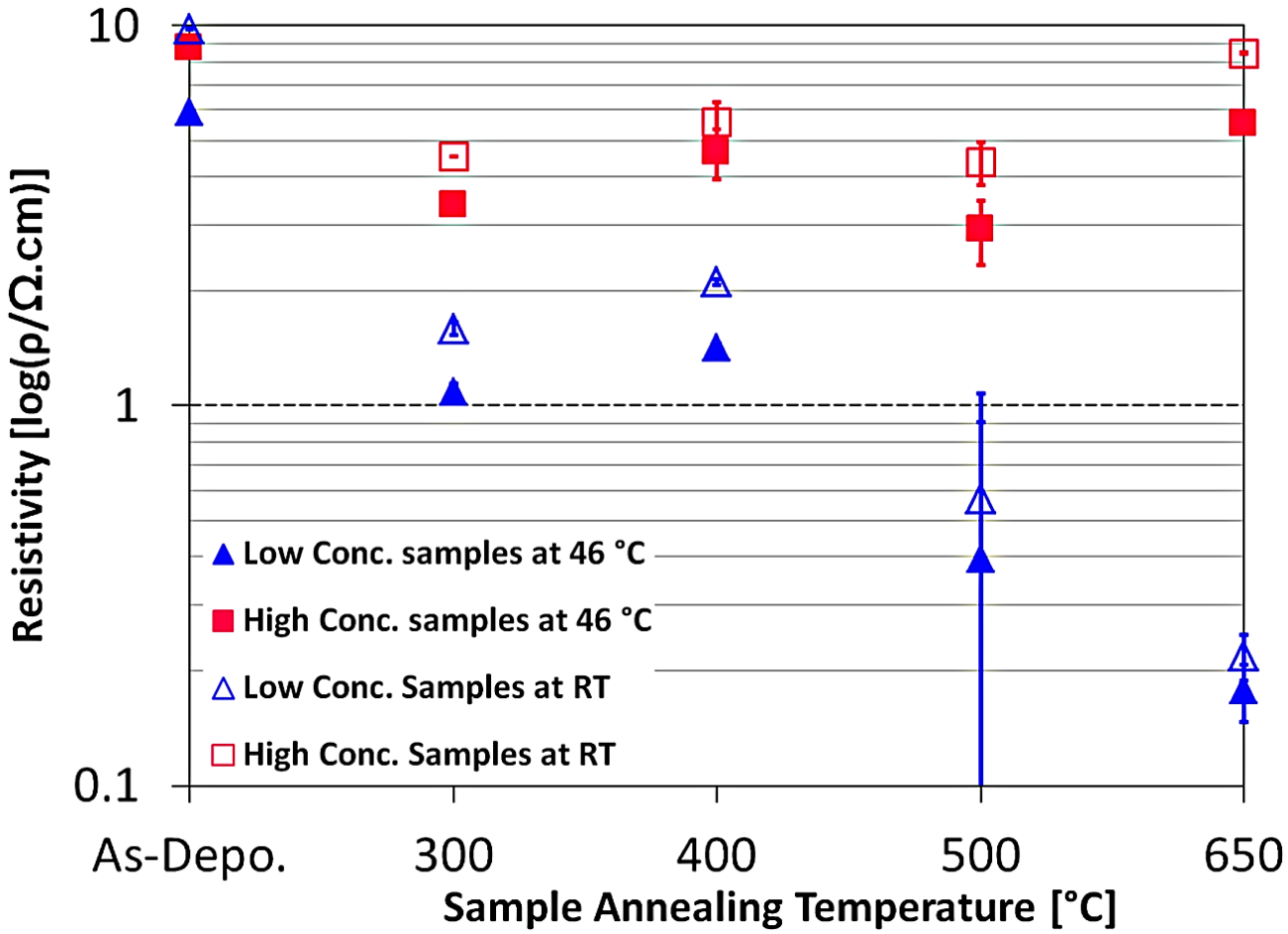

Figure 6 Resistivity of low concentration and high concentration samples at 46ºC as a function of the annealing temperature. The high concentration samples follow a general increasing trend whereas the low concentration samples electrical resistance drops as a function of the annealing temperature.

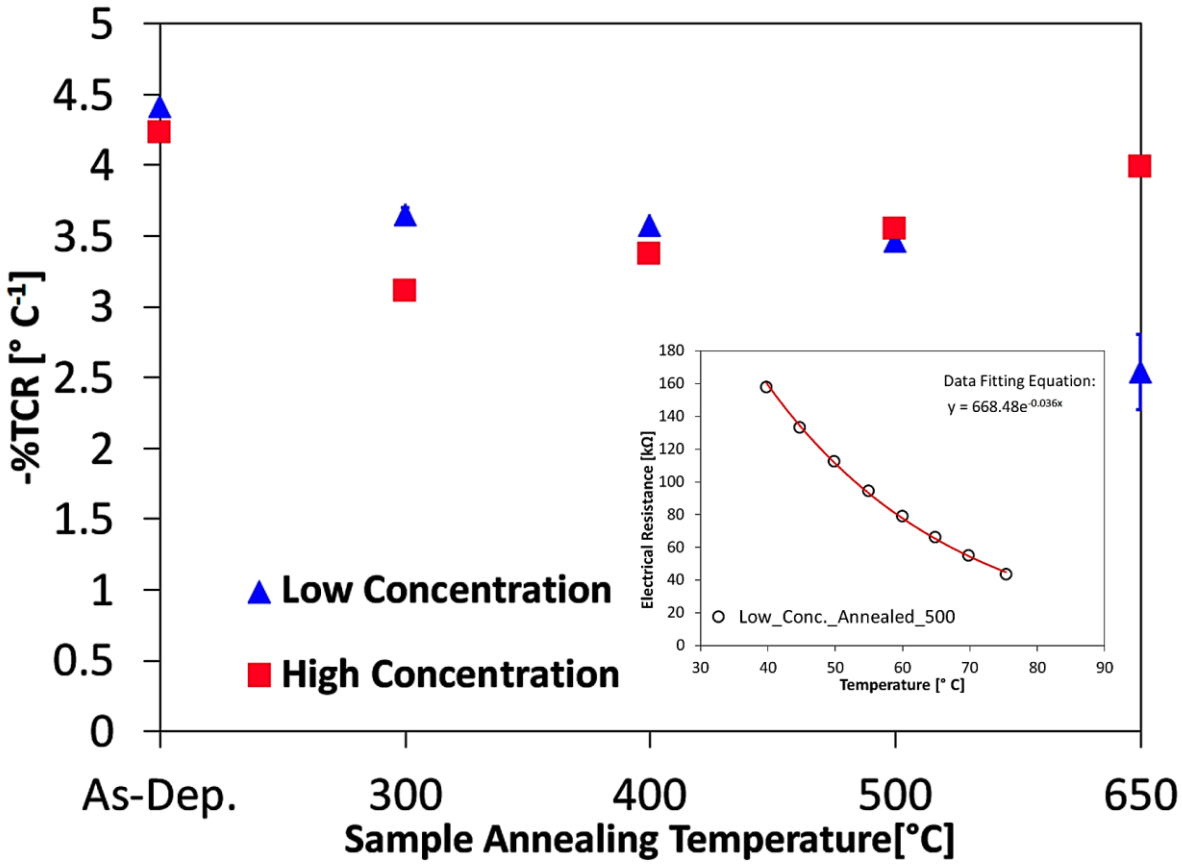

Figure 7 The TCR of the low-concentration and high-concentration samples at 46°C as a function of the sample's annealing temperature. The inset shows the exponential fit to the measurements for one of the low concentration samples annealed at 500°C.